Calculation of Ionization Potentials of Small Molecules: A Comparative Study of Different Methods

Virginie Lemierre,[†] Anna Chrostowska,*[,†] Alain Dargelos,[†] and Henry Chermette*[,‡]

Laboratoire de Physico-Chimie Moléculaire - UMR 5624 - FR 2606, CNRS - Université de Pau et des Pays de l'Adour, Av. de l'Université, BP 1155, 64013 Pau Cedex, France, and Laboratoire de Chimie Physique Théorique - UMR 5182, Université Claude Bernard Lyon-1, 43, Boulevard du 11 Novembre 1918, 69622 Villeurbanne Cedex, France

Received: January 14, 2005; In Final Form: May 10, 2005

With the help of various theoretical methods, ionization potentials (IPs) have been computed for a panel of small molecules containing atoms of group 14, 15, or 16 and representing different singly, doubly, or triply bonded systems with or without an interacting heteroatom lone pair. Comparison of experimental IP values to theoretical results indicates that (i) the standard outer valence green function (OVGF), density functional theory (DFT), and ΔSCF methods lead to rather accurate values, (ii) the CASPT2 method systematically underestimates IPs, (iii) the method of deducing IPs from a shift of some standard DFT eigenvalue spectrum is a straightforward approach leading to rather accurate IPs, (iv) the eigenvalue spectrum obtained with the so-called statistical average of different orbital model potential (SAOP) exchange-correlation model potential is an efficient approach leading directly to quite accurate IPs, and (v) a good prediction of the IP spectrum can be obtained from the shifted excitation spectra of the system calculated by the time-dependent DFT (TD-DFT) method. It is also shown that the TD-DFT calculations of the ionized species bring a significant improvement over the calculations of the neutral molecules, indicating that a great part of the electronic relaxation is already taken into account (in a similar way for all ionizations). Finally, in the case of TD-DFT calculations of neutral molecules, the statistical average of different orbital model potential (SAOP) functional does not lead to significantly better results than the B3LYP functional.

Ultraviolet photoelectron spectroscopy (UPS) was developed in the early 1960's mainly by Turner and Baker.[1] Since that time, important progress have been made, but the aim of this technique remains the determination of accurate values of ionization energies and to use these data to investigate the electronic structure of molecules and ions in the gas phase, particularly short-lived ones. For a reliable assignment of UV photoelectron spectroscopic bands and for the interpretation of spectra, a theoretical approach is more than necessary.

In one of our previous works,[2] experimental results were compared to the values issued from MP2 and density functional theory (DFT) calculations of ionization potentials (IPs). This study was realized on molecules containing main group 14, 15, and 16 elements with different functionals belonging to the LDA, GGA, and hybrid classes (SVWN, BP86, B3P86, B3LYP, and B3PW91). Interest of DFT application has been observed with improvement of the results compared to the MP2 method. However, only the first and second (when possible) IPs were taken into account, but for a reliable interpretation of photoelectron (PE) spectra, the estimation of the following ionization energies as well as their nature brings useful arguments for unambiguous attribution of PE bands.

Therefore, the problem is to select the best method for IP evaluation, considering that the quality of results depends strongly on the nature and size of the studied molecules and that the computation cost and time have to be taken into account as well.

In this work, different types of small molecules containing atoms of group 14, 15, or 16 and representing different singly, doubly, or triply bonded systems with or without an interacting heteroatom lone pair have been chosen. Comparison of results obtained through standard DFT, time-dependent DFT (TD-DFT), the outer valence green function (OVGF) method, the CASPT2 method, and straightforward "corrected" IPs (obtained by a uniform shift (see Computational Details) of the Kohn−Sham (KS) molecular orbital (MO) eigenvalues of the ground state orbitals of the molecule) should constitute an interesting tool for every PE study. The use of Kohn−Sham orbitals for the prediction of ionization energies is traditionally questioned because they were historically introduced by Kohn and Sham as meaningless auxiliary quantities for calculating the densities.[3,4] Indeed, they are in fact the best orbitals one can obtain within a single Slater determinant wave function.[5,6] Their efficient use for reactivity mechanism studies as well as the calculation of various one electron properties has been emphasized by Baerends and others at many occasions.[5−7] In a recent work, Hamel et al.[8] showed that the Kohn−Sham orbitals do indeed provide a good momentum distribution for the interpretation of electron momentum spectra.

However, approximate exchange-correlation (potential) functionals used in standard DFT computations for the calculation of orbitals are known to fall off too rapidly with respect to a $1/r$ asymptote. In consequence, an electron far from the electronic system experiences a full Hartree potential of N electrons instead of the correct one for $N - 1$ electrons. This is

* To whom correspondence should be addressed. E-mail: anna.chrostowska@univ-pau.fr (A.C.); chermet@in2p3.fr (H.C.).
[†] Université de Pau et des Pays de l'Adour.
[‡] Université Claude Bernard Lyon-1.

10.1021/jp050254c CCC: $30.25
Published on Web 08/27/2005

the so-called self-interaction error which, in some typical cases, can lead to artifacts like the spurious dissociation behavior of two-center/three-electron systems.[9] Consequently, the DFT orbital energies severely underestimate the ionization energies they should approximate (at least the highest occupied molecular orbital (HOMO) energy should equal the first IP; see below). Nevertheless, the eigenvalue pattern of a DFT calculation, as providing a rather realistic, if not accurate, description of the ionization spectrum, has been used for a long time, starting at the historical time of the X-alpha approximation.[10,11] On the other hand, it has been recently shown[12,13] that, provided one knows the exact KS potential, which may be constructed from ab initio accurate densities, the KS orbital energies can be identified as approximate but accurate vertical relaxed IPs. In the case of the HOMO, the identification is exact and established a long time ago.[14] The extension of the identification of KS eigenvalues to IPs for open-shell systems has been established recently by Baerends et al.[15]

In this work, we will compare ionization energies obtained through three schemes derived from DFT:

(i) The first one is the crude eigenvalue pattern given by a standard, approximate, widely used exchange-correlation (XC) functional, namely, the B3LYP hybrid functional.[16] The pattern will then be rigidly shifted in order to fit the first IP. As already said, shifted orbital energies have in the past provided an excellent first approximation to experimental IPs.[11]

(ii) The second one is the eigenvalue pattern given by a modified XC potential, namely, the statistical average of different orbital model potential (SAOP) model potential.[17] This potential has the nice features of providing in the large r region a potential with the correct asymptotic Coulombic $1/r$ behavior delivered by the LB94 potential[18] and also correctly reproducing the atomic shell structure in the inner regions, a behavior delivered by the GLLB potential.[19] This leads to substantially downshifted occupied orbital energies. In 2002, the authors already obtained a reasonable agreement between the SAOP orbital energies and 406 experimental IPs of 64 molecules,[12] with an average deviation of 0.4 eV and a maximum deviation of 1.5 eV.

(iii) Finally, the third one is a derivation of the ionization spectrum from the excitation spectrum of the ionized species calculated within the TD-DFT approach. TD-DFT has recently become a reliable method for the calculation of excited state energies and has proven useful in the assignment of electronic states to absorption spectra.[4,20] We will attempt to forward this TD-DFT efficiency to (photo)ionization spectroscopy, assuming that most of the characteristics of a photoelectron are already present in photoexcited electronic transitions.

The remainder of this paper is organized as follows: In the first paragraph, the computational details will be given, and the comparison with experimental data will then be given for the studied compounds gathered in three classes according to their belonging to element group 14, 15, or 16. The detailed theoretical data will not be reported, and only the deviation with respect to experiment will be given in the corresponding tables. Some concluding remarks derived from the comparison of the different approaches will then be given in the last paragraph.

I. Theoretical Background and Computational Details

DFT[4,21] calculations were performed using Gaussian 98[22] and ADF 2004[23] codes, whereas the MOLCAS[24] program package was used for CASPT2 calculations. Geometry optimizations were carried out at the B3LYP[16]/6-311G(d,p) level of theory and were followed by frequency calculations in order to verify that the stationary points obtained were true energy minima. All IP estimations are based on geometries obtained with B3LYP/6-311G(d,p). Triple-ζ + polarization (TZP) STO functions were retained as the orbital basis set for ADF calculations, in all electron calculations (i.e., no frozen core approximation for the core orbitals).

Excited states may be obtained from density functional theory by its time-dependent development.[25] TD-DFT is becoming very popular because of its efficiency for excited state calculation and its reasonable computational cost. We have chosen to take the assignment of the theoretical absorption spectra as a reference for the location of the ionized states. More precisely, provided that the Tamm−Dancoff approximation delivers excited state transition energies dominated by a single orbital excitation (e.g., 0.65 of the oscillator strength), the relative position of the ionization energies is deduced from the transition energies from occupied orbitals to a given virtual orbital. Indeed, there is nothing fundamentally limiting TD-DFT to the treatment of singly excited states if the ground state functional is exact and the frequency dependence of the exchange-correlation kernel is treated, but this is typical of current implementations in most software. In this work, the TD-DFT spectra of the ionized species have been calculated; that is, one assumes that the main relaxation of the orbitals is already taken into account through the first ionization and that this relaxation remains unchanged in the further ionizations. Accordingly, the present calculations are based on the evaluation of the electronic spectrum of the low-lying ions, described by the ΔSCF corresponding to the first vertical ionization potential, IP_{1v}^{calcd}, calculated as the difference $E_{cation} - E_{neutral\ molecule}$.

One has to emphasize that such a TD-DFT approach should be considered as a crude approximation of the spectrum, since the method in its present form describes only single excitations, whereas double excitations should be important in open-shell systems such as the ions studied in the present work.[20] However, some TD-DFT excitation spectra of open-shell molecules have appeared in the past,[26] whereas, in the case of a significant presence of a double excitation within a state, the time-dependent response theory may break down.[27]

Meanwhile, the TD-DFT spectrum of the neutral species has also been calculated, to separate the contribution of the electron relaxation during the ionization process. Indeed, in the case of no significant change between the relative energies of the neutral and ionized excited states, one could conclude that only the ground state electronic spectrum is needed to deduce the full ionization spectrum, provided the first ionization is known: this could be achieved either via experimental data or through a ΔSCF calculation, as already said. Indeed, we will see that in most cases the TD-DFT of neutral species does not provide as good results as the TD-DFT of cations: this could be expected, since low lying states of the ion would not correspond to excitations of the neutral, but this had to be tested, also because some software does not provide (yet) TD-DFT spectra of open-shell systems.

The vertical IPs were also calculated at the ab initio level employing the outer valence green function (OVGF)[28] method in the Gaussian calculation, which includes electron correlation and electron relaxation effects. This method has the advantage of giving results from a single calculation.

CASPT2 refers to multiconfigurational SCF ab initio calculations in which all excitations are taken into account within an orbital space (namely, the active space) fixed to CAS(12,12) in this work, with second-order perturbation corrections added afterward.

TABLE 1: Deviation from Experimental IPs Given for Each Method for $GeCl_2$ and $GeBr_2$[a]

	IP#	symm C_{2v}	exptl IPs[26]	TD-DFT (B3LYP) cation	TD-DFT (B3LYP) GS	TD-DFT (SAOP) GS	OVGF	CASPT2	$-\epsilon_i^{KS}$(B3LYP) (corrected IPs)	$-\epsilon_i^{KS}$ (SAOP)
$GeCl_2$	IP_1	A_1	10.55(n_{Ge})	−0.01*	−0.01*	−0.01*	−0.29	−0.38	−2.38 [/]	0.66
	IP_2	B_2	11.44($n_{Cl}^{\sigma-}$)	−0.32	−0.60	−0.80	−0.19	−0.37	−2.67 [−0.29]	0.26
	IP_3	A_2	11.70($n_{Cl}^{\pi-}$)	−0.32	−0.10	−0.29	−0.15	−0.55	−2.58 [−0.20]	0.36
	IP_4	B_1	12.58($n_{Cl}^{\pi+}$)	−0.54	−0.29	−0.47	−0.3	−0.74	−2.81 [−0.43]	0.07
	IP_5	A_1	12.69($n_{Cl}^{\sigma+}$)	−0.38	−0.66	−0.86	−0.17	−0.58	−2.78 [−0.40]	0.05
$GeBr_2$	IP_1	A_1	10.02(n_{Ge})	−0.11*	−0.11*	−0.11*	−0.32	−0.39	−2.35 [/]	0.71
	IP_2	B_2	10.54($n_{Br}^{\sigma-}$)	−0.26	−0.48	−0.62	−0.18	−0.30	−2.53 [−0.18]	0.43
	IP_3	A_2	10.86($n_{Br}^{\pi-}$)	−0.36	−0.06	−0.26	−0.22	−0.56	−2.52 [−0.17]	0.45
	IP_4	B_1	11.67($n_{Br}^{\pi+}$)	−0.54	−0.21	−0.36	−0.33	−0.37	−2.70 [−0.35]	0.21
	IP_5	A_1	11.82($n_{Br}^{\sigma+}$)	−0.39	−0.59	−0.72	−0.23	−0.51	−2.67 [−0.32]	0.18
	σ			**0.40**	**0.43**	**0.59**	**0.25**	**0.49**	**[0.31]**	**0.40**

[a] All values are in eV. An asterisk represents deviation for the ΔSCF value. Deviation = theoretical value − experimental value. σ is the standard deviation. GS is the ground state of the neutral molecule.

In the present work, we have used two exchange-correlation potentials for the DFT calculations, namely, the B3LYP one[16] in the Gaussian calculation and the model potential SAOP, recently introduced by Baerends and co-workers[17] for TD-DFT applications, in the ADF calculation. So-called corrected IPs were calculated by applying a uniform shift ($x = IP_v^{exptl} + \epsilon^{KS}(HOMO)$), where $\epsilon^{KS}(HOMO)$ is the highest occupied B3LYP/3-111G(d,g) Kohn−Sham MO energy of the ground state molecule and IP_v^{exptl} is the lowest experimental IP energy of the molecule, as suggested previously by Stowasser and Hoffman.[5] The quality of the SAOP XC functional permits us to compare directly eigenvalues of the ground state orbital (obtained with this exchange-correlation potential) to experimental IPs. TD-DFT calculations were performed with both the B3LYP (10 first excitations) and SAOP functionals for the neutral molecules and the B3LYP functional for the ionized species.

II. Results

A. Compounds Containing Main Group 14 Elements. *$GeCl_2$ and $GeBr_2$.* Dihalogenogermylenes are unstable species, which have to be studied with a short-lived species detection technique, such as UV photoelectron spectroscopy. Dichlorogermylene geometrical parameters optimized with the B3LYP/6-311G(d,p) level of theory ($R_{GeCl} = 2.220$ Å, $\theta_{ClGeCl} = 100.5°$) are in quite good agreement with the X-ray diffraction bond length ($R_{GeCl} = 2.183$ Å, $\theta_{ClGeCl} = 100.3°$).[29] $GeCl_2$ and $GeBr_2$ were generated[30] using mixtures consisting of excess crystalline GeS and $PbCl_2$ or $PbBr_2$ in the PE spectrometer (reaction temperature ∼300 °C). For dichlorogermylene, the first ionization potential at 10.55 eV has been assigned to the $4a_1$ MO corresponding to the radial combination of chlorine p AOs destabilized through an antibonding interaction with the germanium sp hybrid orbital. The bands at 11.44, 11.70, 12.58, and 12.69 eV correspond to chlorine lone pair ionizations. The same assignments have been done for dibromogermylene (n_{Ge}: 10.02 eV; n_{Br}: 10.54, 10.86, 11.69, and 11.82 eV). Table 1 lists the deviations (defined as (theoretical value − experimental value)) from experimental data obtained for $GeCl_2$ and $GeBr_2$ with the TD-DFT, OVGF, or CASPT2 approach or by "correcting" calculated Kohn−Sham energies (B3LYP). (Raw) Eigenvalues of (ground state) molecular orbitals obtained with the SAOP are also displayed. Except the first IP calculated by the ΔSCF method, which gives pretty close results ($GeCl_2$: ΔSCF = 10.54, exptl 10.55; $GeBr_2$: ΔSCF = 9.91, exptl 10.02 eV), all others fit less accurately compared with the experimental IPs. The most disappointing is the CASPT2 calculation with always underestimated values. CCSD(T) calculations of the first three cations of $GeCl_2$ have been carried out to approve this tendency. IPs issued from these calculations (10.16 eV (A1), 11.02 eV (B2), and 11.32 eV (A2)) are systematically underestimated by 0.4 eV compared with the experimental values.

B. Compounds Containing Main Group 15 Elements. *1. H_3C-NH_2, H_3C-PH_2, and H_3C-AsH_2.* The calculated geometrical parameters for methylamine CH_3NH_2 ($R_{C-N} = 1.466$ Å, $\theta_{CNH} = 110.1°$) agree very closely with the experimental geometry of Takagi and Kojima ($R_{C-N} = 1.4714$ Å, $\theta_{CNH} = 110.27°$).[19] The well-known photoelectron spectrum of methylamine[20] presents five bands at 9.65 eV (n_N), 13.20 eV (π_{CH_3}), 14.30 eV (σ_{C-N}), 15.30 (π_{CH_3}), and 16.7 eV (π_{NH_2}). In a recent work, Hae-Won Kim reported a theoretical study of the infrared spectrum of methylphosphine CH_3PH_2.[21] Theoretically predicted in this work, the MP2 and DFT/B3LYP level of theory with 6-311G(d,p) basis set results are in close agreement with experimental geometry.[22] Methylphosphine and methylarsine have also been characterized by photoelectron spectroscopy,[20] and in both cases, the first IPs (CH_3PH_2, 9.62 eV; CH_3AsH_2, 9.50 eV) have been associated with the ejection of an electron from the phosphorus and the arsenic lone pair, respectively. For methylarsine, the next bands are due to ionization of the σ_{As-C} bond. Deviations from experimental values are listed in Table 2. For CH_3NH_2, CASPT2, and OVGF, corrected IPs fit better with experimental values than TD-DFT ones, but TD-DFT strongly underestimates these ionization energies (from 0.10 to 0.57 eV). Quite good agreement is noted for methylarsine CASPT2 and corrected values, since the deviation does not exceed 0.17 eV.

2. $H_2C=NH$, $H_2C=PH$, and $H_2C=AsH$. The B3LYP/6-311G-(d,p) methylimine optimized geometry ($R_{C=N} = 1.266$ Å, $\theta_{CNH} = 110.5°$) reproduces correctly experimental values[35] ($R_{C=N} = 1.273$ Å, $\theta_{CNH} = 110.4°$). The photoelectron spectrum of this species has been described by Bock and Dammel.[36] For phosphaethene, geometrical parameters (B3LYP/6-311G(d,p): $R_{C=P} = 1.670$ Å, $\theta_{CPH} = 97.7°$) are also in very good agreement with experimental data[37,38] ($R_{C=P} = 1.673$ Å, $\theta_{CPH} = 97.4°$). Phosphaethene was generated by dehydrochlorination of chloromethylphosphine by the vacuum gas solid reaction[39] (VGSR) and characterized by photoelectron spectroscopy.[40] The first PE band at 10.3 eV is assigned to the ionization of the phosphorus−carbone π double bond ($\pi_{P=C}$) and the second one at 10.7 eV to the phosphorus lone pair (n_P). Recently, vertical ionization energies of phosphaethene have been calculated by M. T.

TABLE 2: Deviation from Experimental IPs Given for Each Method for CH_3NH_2, CH_3PH_2, and CH_3AsH_2[a]

	IP#	symm C_s	exptl IPs[26]	TD-DFT (B3LYP) cation	TD-DFT (B3LYP) GS	TD-DFT (SAOP) GS	OVGF	CASPT2	$-\epsilon_i^{KS}$(B3LYP) (corrected IPs)	$-\epsilon_i^{KS}$ (SAOP)
CH_3NH_2	IP_1	A′	9.65(n_N)	−0.10*	−0.10*	−0.10*	−0.19	−0.27	−3.28 [/]	0.20
	IP_2	A″	13.20(π_{CH_3})	−0.57	−0.08	−0.49	0.16	0.09	−3.20 [0.08]	−0.20
	IP_3	A′	14.30(σ_{C-N})	−0.48		−0.64	−0.14	−0.18	−3.39 [−0.11]	−0.40
	IP_4	A″	15.30(π_{CH_3})	−0.21		−0.57	−0.12	−0.12	−3.38 [−0.10]	−0.42
	IP_5	A″	16.70 (π_{NH_2})	−0.18		−0.76	0.11	0.11	−3.45 [−0.17]	−0.54
CH_3PH_2	IP_1	A′	9.62(n_P)	0.07*	0.07*	0.07*	−0.15	−0.26	−2.62 [/]	0.27
CH_3AsH_2	IP_2	A′	9.50(n_{As})	0.21*	0.21*	0.21*	−0.03	−0.12	−2.43 [/]	0.58
	IP_3	A′	11.65(σ_{C-As})	0.00	0.07	0.05	0.12	0.01	−2.45 [−0.02]	0.40
	IP_4	A″	12.02 (π_{AsH_2})	−0.03	−0.25	−0.34	0.37	0.15	−2.51 [−0.08]	0.26
	σ			**0.32**	**0.16**	**0.53**	**0.18**	**0.16**	**[0.10]**	**0.39**

[a] All values are in eV. An asterisk represents deviation for the ΔSCF value. σ is the standard deviation. GS is the ground state of the neutral molecule.

TABLE 3: Deviation from Experimental IPs Given for Each Method for CH_2NH, CH_2PH, and CH_2AsH[a]

	IP#	symm C_s	exptl IPs[26]	TD-DFT (B3LYP) cation	TD-DFT (B3LYP) GS	TD-DFT (SAOP) GS	OVGF	CASPT2	$-\epsilon_i^{KS}$(B3LYP) (corrected IPs)	$-\epsilon_i^{KS}$ (SAOP)
$CH_2{=}NH$	IP_1	A′	10.60(n_N)	−0.02*	−0.02*	−0.02*	−0.14	−0.34	−3.19 [/]	0.22
	IP_2	A″	12.50($\pi_{C=N}$)	−0.11	1.82	1.89	−0.29	−0.24	−3.33 [−0.14]	0.16
	IP_3	A′	14.80(σ_{C-N})	0.35	−0.05	−0.36	0.22	0.06	−3.05 [0.14]	−0.03
	IP_4	A′	16.90(σ_{C-H})	0.22	−0.19	−0.59	0.23	−0.06	−3.14 [0.05]	−0.22
$CH_2{=}PH$	IP_1	A″	10.30($\pi_{C=P}$)	0.00*	0.00*	0.00*	−0.33	−0.21	−2.71 [/]	0.40
	IP_2	A′	10.70(n_P)	−0.16	−1.54	−1.67	−0.39	−0.7	−2.88 [−0.17]	0.03
	IP_3	A′	13.20(σ_{C-P})	0.15	−1.83	−1.96	0.01	−0.15	−2.73 [−0.02]	−0.02
	IP_4	A′	15.00(σ_{C-H})	0.01	−1.75	−1.99	0.14	−0.07	−2.61 [0.1]	0.00
$CH_2{=}AsH$	IP_1	A″	9.70($\pi_{C=As}$)	0.02*	0.02*	0.02*	−0.18	−0.01	−2.56 [/]	0.60
	IP_2	A′	10.40(n_{As})	−0.03	−1.46	−1.60	−0.18	−0.27	−2.64 [−0.08]	0.35
	IP_3	A′	12.60(σ_{C-As})	0.03	−1.84	−2.02	0.04	−0.07	−2.67 [−0.11]	0.10
	IP_4	A′	14.70(σ_{C-H})	0.04	−1.85	−2.12	0.15	−0.08	−2.57 [−0.01]	0.04
	σ			**0.16**	**1.43**	**1.69**	**0.22**	**0.26**	**[0.10]**	**0.25**

[a] All values are in eV. An asterisk represent deviation for the ΔSCF value. σ is the standard deviation. GS is the ground state of the neutral molecule.

Nguyen[38] with the DFT method including the BLYP and B3LYP functionals, second-order perturbation theory (MP2), quadratic configuration interaction (QCISD(T)) and coupled cluster theory (CCSD(T)). The DFT approach using the B3LYP functional has given results comparable to higher quality methods. Very recently, we have reported the synthesis of methylenearsane by the dehydrohalogenation of chloromethylarsane in a VGSR reaction and its characterization by mass spectrometry and UV photoelectron spectroscopy.[41] Assignments of IPs (9.7 eV ($\pi_{As=C}$), 10.3 eV (n_{As}), 12.6 eV (σ_{C-As}), and 14.7 eV (σ_{C-H})) have been done on the basis of the theoretical support. The reliability of the TD-DFT approach compared to the OVGF and CASPT2 methods or correcting of calculated Kohn−Sham energies has been evidenced. Table 3 lists the deviation from experiment for these unsaturated heterocompounds. Corrected and TD-DFT IPs are found to give better results compared to OVGF and CASPT2 ones. The last one underestimates strongly (−0.70 eV) the second IP value of phosphaethene.

3. $CH_3C{\equiv}N$, $CH_3C{\equiv}P$, and $CH_3C{\equiv}As$. The B3LYP/6-311-(d,p) geometrical parameters calculated for acetonitrile, phosphapropyne, and ethylidynearsine reproduce pretty well experimental structures published by M. Le Guennec et al.,[42] H. W. Kroto et al.,[43] and J. C. Guillemin et al.,[44] respectively. These three molecules have been characterized by PES: $CH_3C{\equiv}N$:[45] 12.21 eV ($\pi_{C\equiv N}$), 13.14 eV (σ_{C-N}), 16.00 eV (π_{CH_2}); $CH_3C{\equiv}P$:[46] 9.89 eV ($\pi_{C\equiv P}$), 12.19 eV (n_P), 14.70 eV (π_{CH_3}), 15.60 eV (π_{CH_3}); $CH_3C{\equiv}As$:[47] 9.6 eV ($\pi_{C\equiv As}$), 12.1 eV (n_{As}). Table 4 displays a comparison between these values and calculated ones. TD-DFT and corrected IPs agree nicely with photoelectron spectroscopy data; on the contrary, OVGF and CASPT2 are disappointing, especially for the phosphapropyne and ethylidynearsine underestimated values provided by the latter one.

C. Compounds Containing Main Group 16 Elements. *$H_2C{=}O$ and $H_2C{=}S$.* The optimized geometries obtained for formaldehyde (CH_2O) ($R_{C=O}$ = 1.110 Å, θ_{HCO} = 122.3°) and thioformaldehyde (CH_2S) ($R_{C=S}$ = 1.090 Å, θ_{HCS} = 122.1°) are in pretty good agreement with experimental structure parameters.[48,49] These two species were characterized by PES, and the following data have been obtained: CH_2O:[45] 10.88 eV (n_O), 14.50 eV ($\pi_{C=O}$), 16.00 eV (σ_{C-O}), and 16.6 eV (σ_{CH_2}); CH_2S:[50] 9.38 eV (n_S), 11.76 eV ($\pi_{C=S}$), 13.85 eV (σ_{C-S}), and 15.20 eV (σ_{CH_2}). The calculated IP deviation from experiment is reported in Table 5. For these compounds, the conclusions are similar to comments given for the previously described molecules; CASPT2 systematically underestimates IPs. With all of the methods used, an important deviation for the fourth ionization energy is observed.

III. Discussion

Relations of the calculated and experimental values of IPs for each method used in this work have been plotted and are displayed in Figures 1−4. As it has been noted, TD-DFT, OVGF, and corrected IPs agree well with experimental results. For the CASPT2 approach, a general trend is the underestimation of ionization energies. These remarks are nicely visualized with the average and model deviations displayed in Table 6. As can be evidenced by a more detailed comparison of calculated IP values, their underestimation by the CASPT2 method is already present, even more strongly at the CASSCF

TABLE 4: Deviation from Experimental IPs Given for Each Method for $CH_3C{\equiv}N$, $CH_3C{\equiv}P$, and $CH_3C{\equiv}As$[a]

	IP#	symm C_{3v}	exptl IPs[26]	TD-DFT (B3LYP) cation	TD-DFT (B3LYP) GS	TD-DFT (SAOP) GS	OVGF	CASPT2	$-\epsilon_i^{KS}$(B3LYP) (corrected IPs)	$-\epsilon_i^{KS}$ (SAOP)
$CH_3C{\equiv}N$	IP_1	E	12.21($\pi_{C\equiv N}$)	0.03*	0.03*	0.03*	0.03	0.03	−3.08 [/]	0.40
	IP_2	A_1	13.14(n_N)	−0.18	0.38	−0.07	−0.08	−0.44	−3.20 [−0.12]	−0.02
	IP_3	E	16.00(π_{CH_3})	−0.31		−0.69	0.10	−0.13	−3.20 [−0.12]	−0.07
$CH_3C{\equiv}P$	IP_1	E	9.89($\pi_{C\equiv P}$)	−0.05*	−0.05*	−0.05*	−0.19	−0.11	−2.62 [/]	0.32
	IP_2	A_1	12.19(n_P)	0.04	2.40	0.07	−0.19	−0.34	−2.63 [−0.01]	0.05
	IP_3	E	14.70(π_{CH_3})	−0.07		−0.54	0.30	−0.03	−2.65 [−0.03]	0.03
	IP_4	A_1	15.60(σ_{C-C})	−0.21		−0.02	0.38	/	−2.21 [0.41]	0.25
$CH_3C{\equiv}As$	IP_1	E	9.60($\pi_{C\equiv As}$)	−0.23*	−0.23*	−0.23*	−0.35	−0.19	−2.78 [/]	0.25
	IP_2	A_1	12.10(n_{As})	−0.06	0.09		−0.35	−0.49	−2.75 [0.03]	0.04
	σ			**0.17**	**1.40**	**0.39**	**0.25**	**0.28**	**[0.18]**	**0.21**

[a] All values are in eV. An asterisk represents deviation for the ΔSCF value. σ is the standard deviation. GS is the ground state of the neutral molecule.

TABLE 5: Deviation from Experimental IPs Given for Each Method for $H_2C{=}O$ and $H_2C{=}S$[a]

	IP#	symm C_{2v}	exptl IPs[26]	TD-DFT (B3LYP) cation	TD-DFT (B3LYP) GS	TD-DFT (SAOP) GS	OVGF	CASPT2	$-\epsilon_i^{KS}$(B3LYP) (corrected IPs)	$-\epsilon_i^{KS}$ (SAOP)
$H_2C{=}O$	IP_1	B_2	10.88(n_O)	−0.09*	−0.09*	−0.09*	−0.10	−0.44	−3.46 [/]	0.16
	IP_2	B_1	14.50($\pi_{C=O}$)	0.09	2.59	1.99	−0.16	−0.15	−3.43 [0.03]	0.13
	IP_3	A_1	16.00(σ_{C-O})	0.18	−0.05	−0.35	0.09	0.00	−3.58 [−0.12]	−0.36
	IP_4	B_2	16.60(σ_{CH_2})	0.67	0.42	−0.20	0.49	0.06	−2.99 [0.47]	0.06
$H_2C{=}S$	IP_1	B_2	9.38(n_S)	−0.01*	−0.01*	−0.01*	−0.37	−0.52	−2.83 [/]	0.09
	IP_2	B_1	11.76($\pi_{C=S}$)	0.06	1.82	1.84	−0.29	−0.19	−2.78 [0.05]	0.22
	IP_3	A_1	13.85(σ_{C-S})	0.30	0.09	0.03	−0.09	−0.24	−2.83 [0.00]	−0.16
	IP_4	B_2	15.20(σ_{CH_2})	0.25	0.30	0.10	0.53	−0.17	−2.31 [0.52]	0.21
	σ			**0.33**	**1.31**	**1.12**	**0.31**	**0.28**	**[0.29]**	**0.19**

[a] All values are in eV. An asterisk represents deviation for the ΔSCF value. Deviation = theoretical value − experimental value. σ is the standard deviation. GS is the ground state of the neutral molecule.

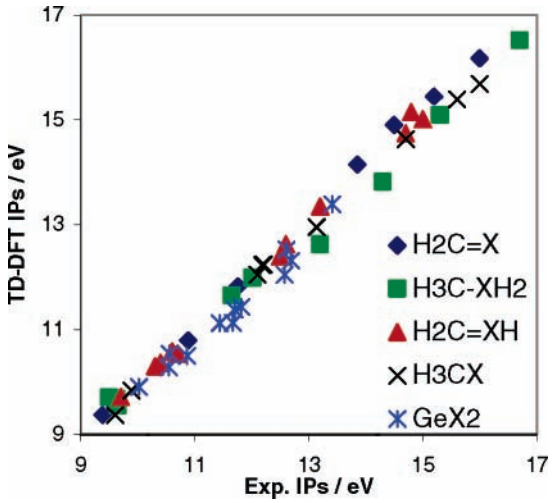

Figure 1. Correlation graph of TD-DFT IPs and experimental IPs for $H_2{=}CX$, CH_3XH_2, $H_2{=}XH$, $CH_3C{\equiv}X$, and GeX_2. Units are in eV (correlation: $y = 1.026x - 0.393$, $R^2 = 0.9884$).

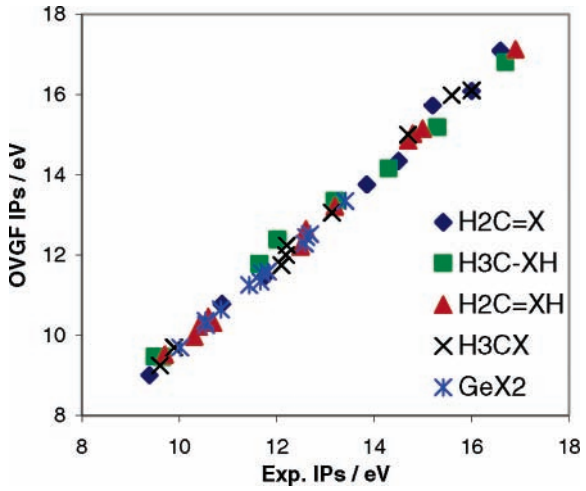

Figure 2. Correlation graph of OVGF IPs and experimental IPs for $H_2{=}CX$, CH_3XH_2, $H_2{=}XH$, $CH_3C{\equiv}X$, and GeX_2. Units are in eV (correlation: $y = 1.073x - 0.998$, $R^2 = 0.9949$).

level. This phenomena might be explained by a lack of balance between the evaluation of the nondynamic correlation energy in the MCSCF level between the neutral molecule (CAS(12,-12)) and the corresponding cation (CAS(11,12)) calculations. Only one part of this missing correlation energy is recovered through the perturbational evaluation of the dynamic correlation energy, so that in this case the average deviation is reduced from −0.3 eV for CASSCF to −0.22 eV for CASPT2. This is coherent with the fact that a range of 0.3 eV error in such a calculation is typical for the CASPT2 method.[51]

The most straightforward, although less rigorous, method which consists of a rigid "shift" of the calculated Kohn−Sham orbital energies of the (first) ionized species toward the first experimental IP provides indeed an excellent first approximation. It comes, probably, from the fact that the electronic relaxation is quite similar for ionizations involving either lone pairs or σ or π molecular bonds. The calculated B3LYP eigenvalues of Kohn−Sham molecular orbitals present an important deviation (∼2 eV) compared to experimental IP values. When these data are corrected, the results improve strongly. Figure 5 represents the correlation graph of eigenvalues of the ground state with the SAOP functional and experimental IPs. The efficiency of this functional compared to more or less standard (GGA, hybrid, like B3LYP) XC functionals is evidenced. One can note the quality of the theoretical spectrum delivered by the (unshifted) eigenvalue spectrum obtained with the SAOP functional. As already said, the corresponding Kohn−Sham potential

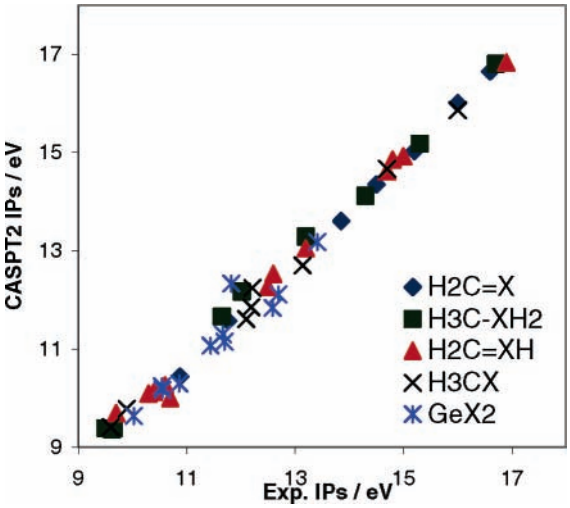

Figure 3. Correlation graph of CASPT2 IPs and experimental IPs for H_2═CX, CH_3XH_2, H_2═XH, CH_3C≡X, and GeX_2. Units are in eV (correlation: $y = 1.042x - 0.729$, $R^2 = 0.9907$).

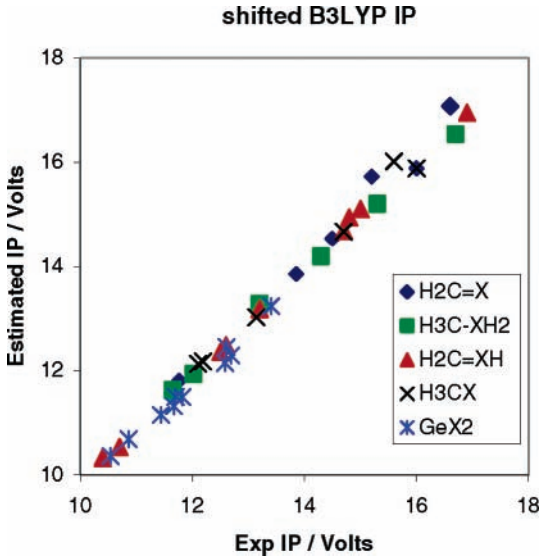

Figure 4. Correlation graph of corrected IPs and experimental IPs for H_2═CX, CH_3XH_2, H_2═XH, CH_3C≡X, and GeX_2. Units are in eV (correlation: $y = 1.056x - 0.805$, $R^2 = 0.9918$).

TABLE 6: Averaged Algebraic Deviation and Standard Deviation from Experimental IPs, Slope of the Regression Line, Given for Each Method (All Values in eV)

method	algeb. differences average	standard deviation	slope
TD-DFT (B3LYP) cation	−0.07	0.29	1.026
TD-DFT (B3LYP) GS	−0.13	1.16	1.052
TD-DFT (SAOP) GS	−0.45	1.06	1.004
OVGF	−0.07	0.24	1.073
CAS	−0.30	0.52	1.077
CASPT2	−0.22	0.32	1.042
corrected IPs (shifted ϵ_i^{KS}(B3LYP))	−0.06	0.21	1.056
ϵ_i^{KS}(SAOP)	−0.14	0.30	0.912
ΔSCF	−0.02	0.10	1.002

contains shape corrections, introduced in order to obtain response properties such as polarizabilities or excitation energies,[52] which lead straightforwardly to orbital eigenvalues close to the corresponding (photo)ionization energies. On the other hand, the eigenvalue spectrum obtained with a simple self-interaction corrected (SIC) functional such as the ADSIC one[53] overcorrects the orbital energies by ∼1 eV. Moreover, in the case of CH_2O, it pushes the b_1 π state much closer to the a_1 state (i.e., 2 eV shift).[54]

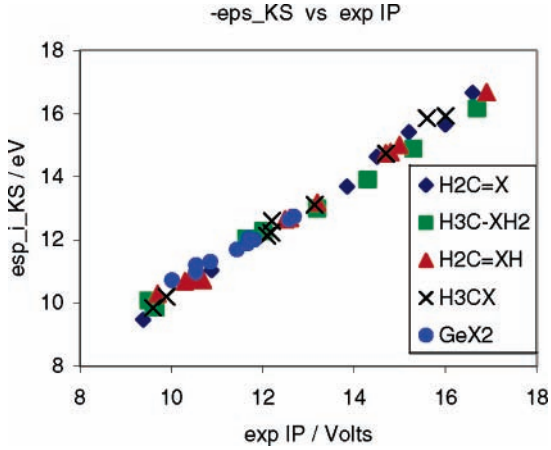

Figure 5. Correlation graph of the first eigenvalues of the ground state orbitals with the SAOP functional and first experimental IPs for H_2═CX, CH_3XH_2, H_2≡XH, CH_3C≡X, and GeX_2. Units are eV (correlation: $y = 0.9124x + 1.2367$, $R^2 = 0.9913$).

According to the Janak theorem,[55] the orbital eigenvalue equals the corresponding ionization potential, and the deviation could be circumvented through two ways:

(i) either the Slater transition state (TS) technique[10] or its generalization by Williams et al.[56] and widely used by Chong et al., Bureau[57,58] or others.

(ii) the use of a modern potential XC functional such as the SAOP[17] used in this work.

Strictly speaking, the ionization energy of the molecular orbital i is given from $-IP = E_N - E_{N-1} = \int_0^1 \epsilon_i \, dn$, where n is the occupation number of the spin−orbital i, and the transition state method comes from the approximation that ϵ_i is supposed to vary linearly with the occupation number, a feature which is rather true in the LDA approximation,[59] so that the integral can be approximated by the eigenvalue for an occupation equal to $^1/_2$.[60,61] Although the main reason of the upper shift of orbital eigenvalues lies in the self-interaction term, this shift may differ between orbitals exhibiting a different localization pattern, in particular σ and π, and this is one of the reasons why a uniform shift of the whole eigenvalue pattern does not exactly fit the ionization spectrum. In the case of a more elaborate potential XC functional, possessing, for example, a correct asymptotic behavior, this self-interaction error is in part taken into account, so that the Slater TS technique is more approximate, and less useful. Another point which could be raised is that the deviations of the theoretical IPs (e.g., through the corrected B3LYP scheme) seem to increase with the ionization energies. We can ascribe this feature to an increase of the localization of inner orbitals, which in turn increases the self-interaction error which is, as just said, the major reason of the upper shift of the orbital eigenvalues of standard Kohn−Sham orbitals (standard = LDA, GGA, and hybrid, like B3LYP but not SAOP). This is indeed an area of active research.[53,54]

The TD-DFT and OVGF approaches allow a good IP estimation, but OVGF takes the advantage to be issued of a single calculation. It is necessary to evaluate the first ionic state by the ΔSCF method (ΔSCF: E_T(cation) − E_T(neutral mol.)) besides TD-DFT calculations. The efficiency of the TD-DFT approximation depends on this value. Figure 6 represents the correlation graph of estimated IPs with the ΔSCF method and experimental ones. These results are in excellent agreement with experiment (average deviation = −0.02 eV and standard deviation = 0.10 eV).

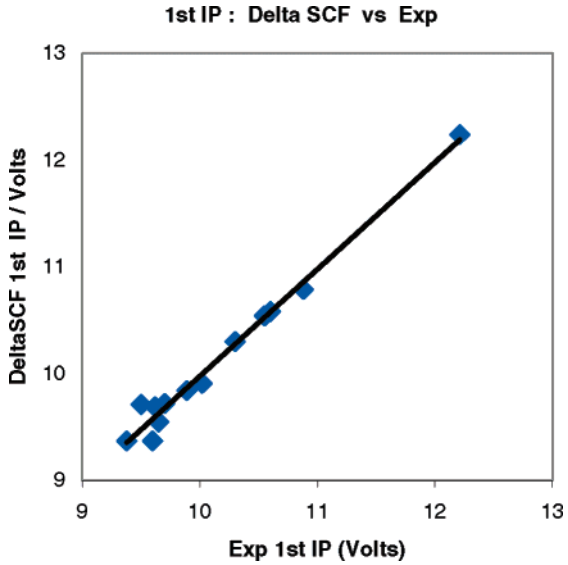

Figure 6. Correlation graph of the first IPs calculated by the ΔSCF method (B3LYP/6−311(d,p)) and first experimental IPs for $H_2{=}CX$, CH_3XH_2, $H_2{=}XH$, $CH_3C{\equiv}X$, and GeX_2. Units are in eV (correlation: $y = 1.002x - 0.037$, $R^2 = 0.9825$).

IV. Concluding Remarks

In this work, ionization potentials have been computed for 13 simple molecules possessing multiple bonds with or without an interacting heteroatom lone pair. Considering all results, we can remark that different methods used in this work for calculating ionization energies lead to rather accurate experimental values, CASPT2 excepted, which systematically underestimates IPs. Both TD-DFT and CASPT2 take the drawback to be "indirect" theoretical approaches in the fact that the first one requires in a first step the calculation of the ion in order to deliver the energy of the fist ionization through a ΔSCF calculation and the second one (CASPT2) needs to do a separate calculation for the neutral species and for the corresponding radical cation. However the calculation of the ion can be efficiently replaced by the use of the experimental, if available, first ionization energy, with the TD-DFT providing then only the relative energies of the subsequent ionizations. These kinds of approaches can be applied only if the first experimental IP is known or can be provided from the PE spectrum without any ambiguity. Of course this situation is more complex when new systems and molecules are studied for the first time and are of important size. Thus, in that case, the good theoretical evaluation of the first IP (and so often the following IPs) becomes crucial.

The direct comparison of experimental IPs to the orbital eigenvalues obtained through calculations using the SAOP XC functional leads to rather accurate IPs (standard deviation 0.30 eV). In agreement with Baerends' observations, the HOMO is found to be slightly too low lying, whereas deeper ionizations are slightly too small (orbital energies too high). Accordingly, the slope of the linear regression, reported in Table 6, is less (by 9%) than 1.0, whereas other approaches lead to slopes larger than 1.0.

One originality of the present work is the attempt to use the time-dependent density functional theory (TD-DFT) theoretical absorption spectra for the prediction of the photoionization spectra. For a spectroscopist, the choice of method has to be done as a function of the efficiency wanted for IP estimation, time, and cost and consequently for photoelectron spectra band analysis and assignment.

Acknowledgment. A.C. and V.L. acknowledge the Conseil Régional d'Aquitaine for financial support for V.L. This work is part of COST Action D26. The CINES is acknowledged for a grant of computer time.

References and Notes

(1) (a) Baker, A. D.; Betteridge, D. *Photoelectron Spectroscopy and Analytical Aspects*; Pergamon Press: Oxford, 1972. (b) Wayne Rabalais, J. *Principles of Ultraviolet Photoelectron Spectroscopy*; John Wiley and Sons: New York, 1977.

(2) Joanteguy, S.; Pfister-Guillouzo, G.; Chermette, H. *J. Phys. Chem. A* **1999**, *103*, 3505. Chermette, H.; Joanteguy, S.; Pfister-Guillouzo, G. In *Recent Advances in Density Functional Methods*; Barone, V., Bencini, A., Fantucci, P., Eds.; World Scientific: Singapore, 2002; Part III, p 91.

(3) Kohn, W.; Sham, L. J. *Phys. Rev.* **1965**, *140*, A1133.

(4) Koch, W.; Holthausen, M. C. *A Chemist's Guide to Density Functional Theory*; Wiley-WCH: Weinheim, Germany, 2000.

(5) Stowasser, R.; Hoffmann, R. *J. Am. Chem. Soc.* **1999**, *121*, 3414.

(6) (a) Gritsenko, O. V.; Baerends, E. J. *J. Phys. Chem. A* **1997**, *101*, 5383. (b) Baerends, E. J.; Gritsenko, O. V.; van Leeuwen, R. In *Application of Density Functional Theory*; Laird, B. B., Ross, R. B., Ziegler, T., Eds.; ACS Symposium Series 629; American Chemical Society: Washington, DC, 1996; pp 20−41.

(7) Gritsenko, O. V.; Ensing, B.; Schipper, P. R. T.; Baerends, E. J. *J. Phys. Chem. A* **2000**, *104*, 8558.

(8) Hamel, S.; Duffy, P.; Casida, M. E.; Salahub, D. R. *J. Electron. Spectrosc. Relat. Phenom.* **2002**, *123*, 345.

(9) (a) Chermette, H.; Ciofini, I.; Mariotti, F.; Daul, C. *J. Chem. Phys.* **2001**, *114*, 1447 and references therein. (b) Chermette, H.; Ciofini, I.; Mariotti, F.; Daul, C. *J. Chem. Phys.* **2001**, *115*, 11068.

(10) Slater, J. C. *Quantum theory of molecules and solids*; McGraw-Hill: New York, 1974; Vol. 4.

(11) (a) Chermette, H.; Pertosa, P.; Michel-Calendini, F. M. *Chem. Phys. Lett.* **1980**, *69*, 240. (b) Michel-Calendini, F.; Chermette, H.; Pertosa, P. *Solid State Commun.* **1979**, *31*, 55. (c) Goursot, A.; Chermette, H.; Daul, C. *Inorg. Chem.* **1984**, *23*, 305. (d) Goursot, A.; Penigault, E.; Chermette, H. *Chem. Phys. Lett.* **1983**, *19*, 215. (e) Chermette, H.; Hollinger, G.; Pertosa, P. *Chem. Phys. Lett.* **1982**, *86*, 170. (f) Perdew, J. P.; Norman, M. R. *Phys. Rev. B* **1982**, *26*, 1884. (g) Godby, R. W.; Schlütler, M.; Sham, L. J. *Phys. Rev. B* **1987**, *36*, 6497. (h) Politzer, P.; Abu-Awwad, F. *Theor. Chem. Acc.* **1998**, *99*, 83.

(12) Chong, D.; Gritsenko, O. V.; Baerends, E. J. *J. Chem. Phys.* 2002, *116*, 1760.

(13) Gritsenko, O. V.; Braıda, B.; Baerends, E. J. *J. Chem. Phys.* **2003**, *119*, 1937.

(14) (a) Perdew, J. P.; Parr, R. G.; Levy, M.; Balduz, J. L. *Phys. Rev. Lett.* **1982**, *49*, 169. (b) Almbladh, C. O.; von Barth, U. *Phys. Rev.* **1985**, *B31*, 3231.

(15) (a) Gritsenko, O. V.; Baerends, E. J. *J. Chem. Phys.* **2002**, *117*, 9154. (b) Gritsenko, O. V.; Baerends, E. J. *J. Chem. Phys.* **2004**, *120*, 8364.

(16) (a) Becke, A. D. *Phys. Rev.* **1988**, *38*, 3098. (b) Becke, A. D. *J. Chem. Phys.* **1993**, *98*, 5648. (c) Lee, C.; Yang, W.; Parr, R. G. *Phys. Rev.* **1988**, *B37*, 785.

(17) (a) Gritsenko, O. V.; Schipper, P. R. T.; Baerends, E. J. *Chem. Phys. Lett.* **1999**, *302*, 199. (b) Schipper, P. R. T.; Gritsenko, O. V.; van Gisbergen, S. J. A.; Baerends, E. J. *J. Chem. Phys.* **2000**, *112*, 1344. (c) Gritsenko, O. V.; Schipper P. R. T.; Baerends E. J. *Int. J. Quantum Chem.* **2000**, *76*, 407.

(18) van Leeuwen, R.; Baerends, E. J. *Phys. Rev. A* **1994**, *49*, 2421.

(19) (a) Gritsenko, O. V.; van Leeuwen, R.; van Lenthe, E.; Baerends, E. J. *Phys. Rev. A* **1995**, *51*, 1944. (b) Gritsenko, O. V.; van Leeuwen, R.; Baerends, E. J. *Int. J. Quantum Chem.* **1997**, *61*, 231.

(20) (a) Casida, M. E.; Salahub, D. R. *J. Chem. Phys.* **2000**, *113*, 8918. (b) Casida, M. E.; Jamorski, C.; Casida, K. C.; Salahub, D. R. *J. Chem. Phys.* **1998**, *108*, 4439. (c) Casida, M. E. *Phys. Rev. A* **1995**, *51*, 2005. (d) Casida, M. E. In *Recent Developments and Applications of Modern Density Functional Theory, Theoretical and Computational Chemistry*; Seminario, J. M., Ed.; Amsterdam, 1996; Vol. 4, p 391. (e) Jamorski, C.; Casida, M. E.; Salahub, D. R. *J. Chem. Phys.* **1996**, *104*, 5134. (f) Bauernschmitt, R.; Ahlrichs, R. *Chem. Phys. Lett.* **1996**, *256*, 454. (g) Petersilka, M.; Gossmann, U. J.; Gross, E. K. U. *Phys. Rev. Lett.* **1996**, *76*, 1212. (h) van Gisbergen, S. J. A.; Koostra, F.; Schipper, P. R. T.; Gritsenko, O. V.; van Gisbergen, S. J. A.; Baerends, E. J. *Phys. Rev. A* **1997**, *57*, 2556. (i) Tozer, D.; Handy, N. C. *J. Chem. Phys.* **1998**, *109*, 10180. (j) Boulet, P.; Chermette, H.; Daul, C.; Gilardoni, F.; Rogemond, F.; Weber, J.; Zuber, G. *J. Phys. Chem. A* **2001**, *105*, 885.

(21) (a) Parr, R. G.; Yang, W. *Density Functional Theory of Atoms and Molecules*; Oxford University Press: New York, 1989. (b) Frish, M. J.; Trucks, G. W.; Cheeseman, J. R. Systematic Model Chemistries Based on Density Functional Theory: Comparison with Traditional Models and with Experiment. In *Recent Development and Applications of Modern Density*

Functional Theory, Theoretical and Computational Chemistry; Seminario, J. M., Ed.; Elsevier Science B. V.: Amsterdam, 1996; Vol. 4, pp 679−707.

(22) Frisch, M. J.; Trucks, G. W.; Schlegel, H. B.; Scuseria, G. E.; Robb, M. A.; Cheeseman, J. R.; Zakrzewski, V. G.; Montgomery, J. A., Jr.; Stratmann, R. E.; Burant, J. C.; Dapprich, S.; Millam, J. M.; Daniels, A. D.; Kudin, K. N.; Strain, M. C.; Farkas, O.; Tomasi, J.; Barone, V.; Cossi, M.; Cammi, R.; Mennucci, B.; Pomelli, C.; Adamo, C.; Clifford, S.; Ochterski, J.; Petersson, G. A.; Ayala, P. Y.; Cui, Q.; Morokuma, K.; Malick, D. K.; Rabuck, A. D.; Raghavachari, K.; Foresman, J. B.; Cioslowski, J.; Ortiz, J. V.; Stefanov, B. B.; Liu, G.; Liashenko, A.; Piskorz, P.; Komaromi, I.; Gomperts, R.; Martin, R. L.; Fox, D. J.; Keith, T.; Al-Laham, M. A.; Peng, C. Y.; Nanayakkara, A.; Gonzalez, C.; Challacombe, M.; Gill, P. M. W.; Johnson, B. G.; Chen, W.; Wong, M. W.; Andres, J. L.; Head-Gordon, M.; Replogle, E. S.; Pople, J. A. *Gaussian 98*, revision A.7; Gaussian, Inc.: Pittsburgh, PA, 1998.

(23) Baerends, E. J.; Autschbach, J.; Bérces, A.; Bo, C.; Boerrigter, P. M.; Cavallo, L.; Chong, D. P.; Deng, L.; Dickson, R. M.; Ellis, D. E.; Fan, L.; Fischer, T. H.; Fonseca Guerra, C.; van Gisbergen, S. J. A.; Groeneveld, J. A.; Gritsenko, O. V.; Grüning, M.; Harris, F. E.; van den Hoek, P.; Jacobsen, H.; van Kessel, G.; Kootstra, F.; van Lenthe, E.; McCormack, D. A.; Osinga, V. P.; Patchkovskii, S.; Philipsen, P. H. T.; Post, D.; Pye, C. C.; Ravenek, W.; Ros, P.; Schipper, P. R. T.; Schreckenbach, G.; Snijders, J. G.; Sola, M.; Swart, M.; Swerhone, D.; te Velde, G.; Vernooijs, P.; Versluis, L.; Visser, O.; van Wezenbeek, E.; Wiesenekker, G.; Wolff, S. K.; Woo, T. K.; Ziegler, T. *ADF2004.01*, SCM; Theoretical Chemistry, Vrije Universiteit: Amsterdam, The Netherlands, http://www.scm.com ADF 2004, release 01, Amsterdam, 2004.

(24) Andersson, K.; Barysz, M.; Bernhardsson, A.; Blomberg, M. R. A.; Cooper, D. L.; Fleig, T.; Fuelscher, M. P.; de Graaf, C.; Hess, B. A.; Karlstroem, G.; Lindh, R.; Malmqvist, P. A. A.; Neogrady, P.; Olsen, J.; Roos, B. O.; Sadlej, A. J.; Schuetz, M.; Schimmelpfennig, B.; Seijo, L.; Serrano-Andres, L.; Siegbahn, P. E. M.; Staalring, J.; Thorsteinsson, T.; Veryazov, V.; Widmark, P. O. *MOLCAS*, version 5; Lund University: Sweden, 2000.

(25) (a) Stratmann, R. E.; Scuseria, G. E.; Frisch, M. J. *J. Chem. Phys.* **1998**, *109*, 8218. (b) Casida, M. E.; Jamorski, C.; Casida, K. C.; Salahub, D. R. *J. Chem. Phys.* **1998**, *108*, 4439.

(26) (a) Guan, J.; Casida, M. E.; Salahub, D. R *THEOCHEM* **2000**, *527*, 229. (b) Hirata, S.; Head-Gordon, M. *Chem. Phys. Lett.* **1999**, *302*, 375.

(27) Neugebauer, J.; Baerends, E. J.; Nooijen, M. *J. Chem. Phys.* **2004**, *121*, 6155.

(28) (a) von Niessen, W.; Schirmer, J.; Cederbaum, L. S. *Comput. Phys. Rep.* **1984**, *1*, 57. (b) Ortiz, J. V. *J. Chem. Phys.* **1988**, *89*, 6348.

(29) (a) Schultz, G.; Tremmel, J.; Hargittai, J.; Berecz, I.; Bohatka, S.; Kagramov, N. D.; Maltsev, A. K, Nefedov, O. M. *J. Mol. Struct.* **1979**, *55*, 207. (b) Vadja, E.; Hargittai, I.; Kolonitz, M.; Ujszaszy, K.; Tamas, J.; Maltsev, A. K.; Mikaelian, R. G.; Nefedov, O. M. J. *Organomet. Chem.* **1976**, *105*, 33.

(30) Jonkers, G.; van der Kerk, S.; de Lange, C. A. *Chem. Phys.* **1982**, *70*, 69.

(31) Takagi, K.; Kojima, T. *J. Phys. Soc. Jpn.* **1971**, *30*, 1145.

(32) Elbel, S.; Diek, H. T.; Demuth, R. *J. Fluorine Chem.* **1982**, 349.

(33) Kim, H. W.; Zeroka, D. *THEOCHEM* **2001**, *571*, 59.

(34) Lannon, J. A.; Nixon, E. R. S*pectrochim. Acta* **1967**, *23A*, 2713 (Ph.D. Thesis of J. A. Lannon, Department of Chemistry, University of PA, 1967).

(35) Pearson, R. G.; Lovas, F. J. *J. Chem. Phys.* **1977**, *66*, 4149.

(36) Bock, H.; Dammel, R. *Chem. Ber.* 1987, *120*, 1961.

(37) Kroto, H. W.; Nixon, J. F.; Ohno, K. *J. Mol. Spectrosc.* **1981**, *90*, 367.

(38) Nguyen, M. T.; Creve, S.; Vanquickenborne, L. G. *J. Chem. Phys.* **1996**, *105*, **1922**.

(39) Guillemin, J. C.; Denis, J. M. *Angew. Chem.* **1982**, *94*, 715; *Angew. Chem., Int. Ed. Engl.* **1982**, *21*, 690; *Angew. Chem Suppl.* **1982**, 1515−1524. For a review on the VGSR technique, see: Vallée, Y. *Gas-Phase Reactions in Organic Synthesis*; Gordon & Breach Science Publishers: New York, **1997**; pp 195−235.

(40) Lacombe, S.; Gonbeau, D.; Cabioch, J. L.; Pellerin, B.; Denis, J. M.; Pfister-Guillouzo, G. *J. Am. Chem. Soc.* **1988**, *110*, 6964.

(41) Chrostowska, A.; Dargelos, A.; Lemierre, V.; Sotiropoulos, J. M.; Guenot, P.; Guillemin, J. C. *Angew. Chem., Int. Ed.* **2004**, *43*, 873.

(42) Le Guennec, M.; Wlodarczak, G.; Burie, J.; Demaison, J. *J. Mol. Spectrosc.* **1992**, *154*, 305.

(43) Kroto, H. W.; Nixon, J. F.; Simmons, N. P. C. *J. Mol. Spectrosc.* **1979**, *77*, 270.

(44) Guillemin, J. C.; Lassalle, L.; Drean, P.; Wlodarczak, G.; Demaison, J. *J. Am. Chem. Soc.* **1994**, *116*, 8930.

(45) Kimura, K.; Katsumata, S.; Achiba, Y.; Yamazaki, T.; Iwata, S. *Handbook of HeI photoelectron Spectra of Fundamental Organic Molecules*; Japan Scientific Societies Press: Tokyo, Halsted Press: New York, 1981; Part II, pp 178 (CH_3CN) and 144 (CH_2O).

(46) Westwood, N. P. C.; Kroto, H. W.; Nixon, J. F.; Simmons, N. P. C. *J. Chem. Soc., Dalton Trans.* **1979**, 1405.

(47) Metail, V.; Senio, A.; Lassalle, L.; Guillemin, J. C.; Pfister-Guillouzo, G. *Organometallics* **1995**, *14*, 4732.

(48) Carter, S.; Handy, N. C. *J. Mol. Spectrosc.* **1996**, *179*, 65.

(49) Turner, P. H.; Halogen, L.; Mills, I. M. *J. Mol. Spectrosc.* **1981**, *88*, 402.

(50) Solouki, B.; Rosmus, P.; Bock, H. *J. Am. Chem. Soc.* **1976**, *98*, 6054.

(51) Tozer, D. J.; Amos, R. D.; Handy, N. C.; Roos, B. O.; Serrano-Andres, L. *Mol. Phys.* **1999**, *97*, 859.

(52) Grüning, M.; Gritsenko, O. V.; van Gisbergen, S. J. A.; Baerends, E. J. *J. Chem. Phys.* **2002**, *116*, 9591.

(53) (a) Ciofini, I.; Chermette, H.; Adamo, C. *Chem. Phys. Lett.* **2003**, *380*, 12. (b) Ciofini, I.; Chermette, H.; Adamo, C. *Chem. Phys.* **2005**, *309*, 67.

(54) Ciofini, I.; Chermette, H. Unpublished data.

(55) Janak, J. F. *Phys. Rev. B* **1978**, *18*, 7165.

(56) Williams, A. R.; deGroot, R. A.; Sommers, C. B. *J. Chem. Phys.* **1975**, *63*, 628.

(57) Hu, C. H.; Chong, D. P. *Chem. Phys. Lett.* **1996**, *262*, 733.

(58) Bureau, C. *Chem. Phys. Lett.* **1997**, *269*, 378.

(59) Makhyoun, M. A.; Le Beuze, A.; Lissillour, R.; Chermette, H. *Theor. Chim. Acta* **1983**, *63*, 383.

(60) Chermette, H. *New J. Chem.* **1992**, *16*, 1081.

(61) Chermette, H. *Coord. Chem. Rev.* **1998**, *178*−*180*, 699.